Immunity
Article

The RIG-I-like Receptor LGP2 Controls CD8+ T Cell Survival and Fitness

Mehul S. Suthar,[1,5] Hilario J. Ramos,[1,5] Margaret M. Brassil,[1] Jason Netland,[1] Craig P. Chappell,[1] Gabriele Blahnik,[1] Aimee McMillan,[1] Michael S. Diamond,[4] Edward A. Clark,[1,2] Michael J. Bevan,[1,3] and Michael Gale, Jr.[1,2,*]
[1]Department of Immunology
[2]Department of Microbiology
[3]The Howard Hughes Medical Institute
University of Washington School of Medicine, Seattle, WA 98195 USA
[4]Departments of Medicine, Molecular Microbiology, and Pathology and Immunology, Washington University School of Medicine, St. Louis, MO 63110, USA
[5]These authors contributed equally to this work.
*Correspondence: mgale@u.washington.edu
http://dx.doi.org/10.1016/j.immuni.2012.07.004

SUMMARY

The RIG-I-like receptors (RLRs) signal innate immune defenses upon RNA virus infection, but their roles in adaptive immunity have not been clearly defined. Here, we showed that the RLR LGP2 was not essential for induction of innate immune defenses, but rather was required for controlling antigen-specific CD8+ T cell survival and fitness during peripheral T cell-number expansion in response to virus infection. Adoptive transfer and biochemical studies demonstrated that T cell-receptor signaling induced LGP2 expression wherein LGP2 operated to regulate death-receptor signaling and imparted sensitivity to CD95-mediated cell death. Thus, LGP2 promotes an essential prosurvival signal in response to antigen stimulation to confer CD8+ T cell-number expansion and effector functions against divergent RNA viruses, including West Nile virus and lymphocytic choriomeningitis virus.

INTRODUCTION

Pathogen recognition and signaling of cell-intrinsic innate immunity is a crucial process for initiation of the immune response to virus infection. Early recognition of RNA viruses and the induction of innate antiviral immunity are largely dependent on the RIG-I-like receptors (RLRs) (Loo et al., 2008). Members of the RLR family of cytosolic RNA helicases, which includes RIG-I, MDA5, and LGP2, are expressed basally at low levels in most tissues and are induced by type I interferon (IFN). RIG-I and MDA5 encode amino-terminal tandem caspase activation and recruitment domains (CARDs) that function in downstream signaling to induce the expression of IFN and other proinflammatory cytokines; in contrast, LGP2 (encoded by *Dhx58*) neither possesses CARDs nor has an analogous signaling effector domain (Yoneyama et al., 2005). Upon binding to RNA pathogen-associated molecular patterns, the RLRs undergo conformational changes and modifications that promote their signaling functions. In particular, RIG-I and MDA5 signal downstream through direct interactions with the MAVS (also known as IPS-1) adaptor protein mediated by CARD-CARD interaction to initiate signaling of the activation of transcription factors IRF-3 and NF-κB. This process induces expression of immune effector genes, IFN, and IFN-stimulated genes (ISGs) that impart innate and adaptive immune defenses to limit virus replication and spread (Wilkins and Gale, 2010). In contrast, LGP2 can function as a negative regulator of RLR signaling by binding viral double-stranded RNA (Rothenfusser et al., 2005), inhibiting RIG-I multimerization (Saito et al., 2007), or competing for a common docking site with IKK-ε on MAVS to suppress innate immune signaling actions (Komuro and Horvath, 2006). More recent studies with *Dhx58*$^{-/-}$ mice have suggested that LGP2 can also function as a positive cofactor of RLR signaling of innate immune defenses (Satoh et al., 2010; Venkataraman et al., 2007), although the exact mechanism by which LGP2 contributes to RIG-I or MDA5 signaling actions remains unknown.

West Nile virus (WNV) is an emerging flavivirus of public health importance and is now a major cause of epidemic encephalitis worldwide (Centers for Disease Control and Prevention (CDC), 2008). RLR signaling and adaptive immune responses are essential for immune protection against WNV infection. Within infected cells, WNV is recognized as a pathogen by the combined actions of RIG-I and MDA5 to temporally induce innate immune responses that are essential in controlling virus replication and modulating B and T cell responses (Fredericksen et al., 2008; Suthar et al., 2010). Whereas humoral immune responses are important for controlling systemic virus infection (Diamond et al., 2003a; Diamond et al., 2003b), cell-mediated responses, specifically those of CD8+ T cells (Brien et al., 2011; Shrestha and Diamond, 2004; Shrestha et al., 2006; Szretter et al., 2010), are critical in controlling virus replication and virus-induced pathology within the CNS. CD4+ T cells play a more prominent role in providing help in development of virus-specific antibody responses and in clearance of WNV from the CNS at later times during infection (Sitati and Diamond, 2006). Regulation of the adaptive immune response is dependent on RLR signaling through MAVS (Suthar et al., 2010). RLR signaling also modulates the quality and balance of the adaptive immune response, including governance of T cell-number expansion,

inflammatory cell infiltration into the CNS, and generation of neutralizing antibodies (Suthar et al., 2010). These observations indicate that RIG-I and MDA5 signaling through MAVS is important for an effective adaptive immune response against virus infection; however, the role of LGP2 in antiviral immunity and pathogenesis of WNV infection has remained poorly understood.

In this study, we generated a *Dhx58*$^{-/-}$ mouse line on a pure C57BL/6 background and evaluated the role of LGP2 in RNA virus infection and immunity. Our results revealed an essential role for LGP2 in promoting CD8^{+} T cell survival and fitness through regulation of sensitivity to death-receptor-mediated cell death. We also confirmed a role for LGP2 function as a positive regulator of RLR signaling of innate immune defenses in primary fibroblasts and myeloid-derived cells ex vivo, and we demonstrated that LGP2 is not essential for induction of innate immunity in lymphoid organs and within the CNS in response to WNV challenge. Importantly, our study defines a cell-intrinsic role for LGP2 in regulation of T cell responses during RNA virus infection and further demonstrates the importance of RLR signaling in regulating immunity and infection.

RESULTS

LGP2 Is Not Required for Innate Defenses but Serves to Enhance RLR-Dependent IFN Induction

To define the role of LGP2 in directing immunity to virus infection, we generated a line of *Dhx58*$^{-/-}$ mice on a pure C57BL/6 background (Figure 1A), thus alleviating confounding variables from mixed genetic background present in existing *Dhx58*$^{-/-}$ mouse lines (Satoh et al., 2010; Venkataraman et al., 2007). We engineered a gene-targeting vector that uniquely replaced *Dhx58* exons 2 to 8, including the translation start codon, with a neomycin cassette. This construct was used to target *Dhx58* in C57BL/6 embryonic stem cells, which were injected into a C57BL/6 donor mouse embryo. Southern blot analysis and quantitative RT-PCR (qRT-PCR) confirmed the deletion of LGP2 (Figure 1B and data not shown, respectively). Progeny mice from *Dhx58*$^{+/-}$ or *Dhx58*$^{-/-}$ intercrosses were born at a normal Mendelian ratio and showed no overt physical defects, in contrast to another *Dhx58*$^{-/-}$ mouse line (Satoh et al., 2010). Expression of LGP2 was not detected in *Dhx58*$^{-/-}$-derived mouse embryo fibroblasts (MEFs) cultured in the presence of IFN (Figure 1C). When infected with Sendai virus (SeV), Dengue virus type 2 (DENV2), or WNV (WNV-TX-02; representing the pathogenic and emerging strain of WNV [Keller et al., 2006]), *Dhx58*$^{-/-}$ MEFs produced slightly reduced amounts of IFN-β but retained temporal induction of IFIT2 and IFIT3 expression (Figure 1D). IFN-β induction by SeV, DENV2, and WNV is dependent on RLR signaling (Loo et al., 2008), and IFIT2 and IFIT3 are ISGs whose expression can be driven acutely by IRF-3 alone (Grandvaux et al., 2002). These results indicate that virus-induced RLR signaling to IRF-3 remains intact but IFN-β induction is moderately attenuated in MEFs in the absence of LGP2.

To determine the role of LGP2 in triggering innate immune defenses in myeloid cells, we evaluated the response of bone-marrow-derived dendritic cells (DCs) and macrophages to WNV infection. Both cell types are targets of WNV infection in vivo (Samuel and Diamond, 2006). *Dhx58*$^{-/-}$ DCs (Figure 1E) and macrophages (Figure 1F) infected with WNV produced reduced amounts of IFN-β compared to wild-type (WT) cells, suggesting a positive regulatory role for LGP2 in facilitating IFN-β production in myeloid cells. In contrast, LGP2 was highly expressed in WT WNV-infected DCs (Figure 1G) and macrophages (Figure 1H), whereas the absence of LGP2 did not alter the expression kinetics or the magnitude of IRF-3 target genes or ISGs, including those that encode RIG-I, MDA5, STAT-1, IFIT2, and IFIT3. We observed significantly higher virus replication at 24 hr postinfection in WNV-infected *Dhx58*$^{-/-}$ DCs (Figure 1I) and macrophages (Figure 1J) compared to WT infected cells. However, by later time points, WT and *Dhx58*$^{-/-}$ infected cells produced similar amounts of infectious virus. Taken together, these results validate LGP2 as a nonessential but positive regulator of RLR signaling of innate immune defenses and demonstrate that it can function to enhance IFN-β production during acute RNA virus infection.

LGP2 Is Essential for Protection against WNV Infection and Virus Control in the CNS

To examine the role of LGP2 in mediating protection against virus infection in vivo, we challenged WT and *Dhx58*$^{-/-}$ mice with WNV (WNV-TX) and assessed clinical phenotype, virologic as well as immunologic responses. Following a subcutaneous inoculation in the footpad, WNV replicates in the popliteal draining lymph node (pDLN), which results in viremia and spread to the spleen and CNS tissues (e.g., brain and spinal cord), thus recapitulating the pathogenesis of human infection (Samuel and Diamond, 2006). *Dhx58*$^{-/-}$ mice were found to be more susceptible to WNV infection (Figure 2A) and exhibited a significant increase in mortality (87.5% compared to 13% in WT mice; $p < 0.0001$) as compared to WT infected mice. Thus, LGP2 is required for protection against WNV infection in vivo.

To begin to define the basis for the increased mortality in *Dhx58*$^{-/-}$ mice, we evaluated the viral burden in different tissues over time. Analysis of virus levels within the pDLN (Figure 2B) and spleen (Figure 2C) revealed no differences in tissue viral load between WT and *Dhx58*$^{-/-}$ infected mice. In contrast to *Mavs*$^{-/-}$ mice (Suthar et al., 2010), *Dhx58*$^{-/-}$ infected mice exhibited normal tissue tropism, with no expansion to organs (e.g., the kidney) that normally are resistant to infection in WT mice. (Figure 2D). Furthermore, comparable peripheral innate immune responses were observed in the absence of LGP2, as evidenced by similar amounts of IFN-β production (Figure 2E) and ISG expression in the pDLN (Figure 2F-G), ISG expression in the spleen (Figure 2H), and type I IFN in the serum (Figure 2I).

Dhx58$^{-/-}$ infected mice displayed similar kinetics of viral neuroinvasion to those of WT infected mice (see day 6, Figure 3A), although significantly higher viral loads were observed in the brain at late time points during infection, indicating that LGP2 is required for controlling virus replication and/or spread after entering the CNS. Accordingly, we examined WNV replication and innate immune defenses in primary cortical neurons isolated from WT or *Dhx58*$^{-/-}$ mice after ex vivo infection. We found that LGP2 was not essential for controlling virus replication in neurons, as WNV reached end-point viral loads in *Dhx58*$^{-/-}$ cortical neurons similar to those of WT neurons (Figure 3B). Furthermore, LGP2 was not required for the induction or enhancement of innate immune defenses against infection

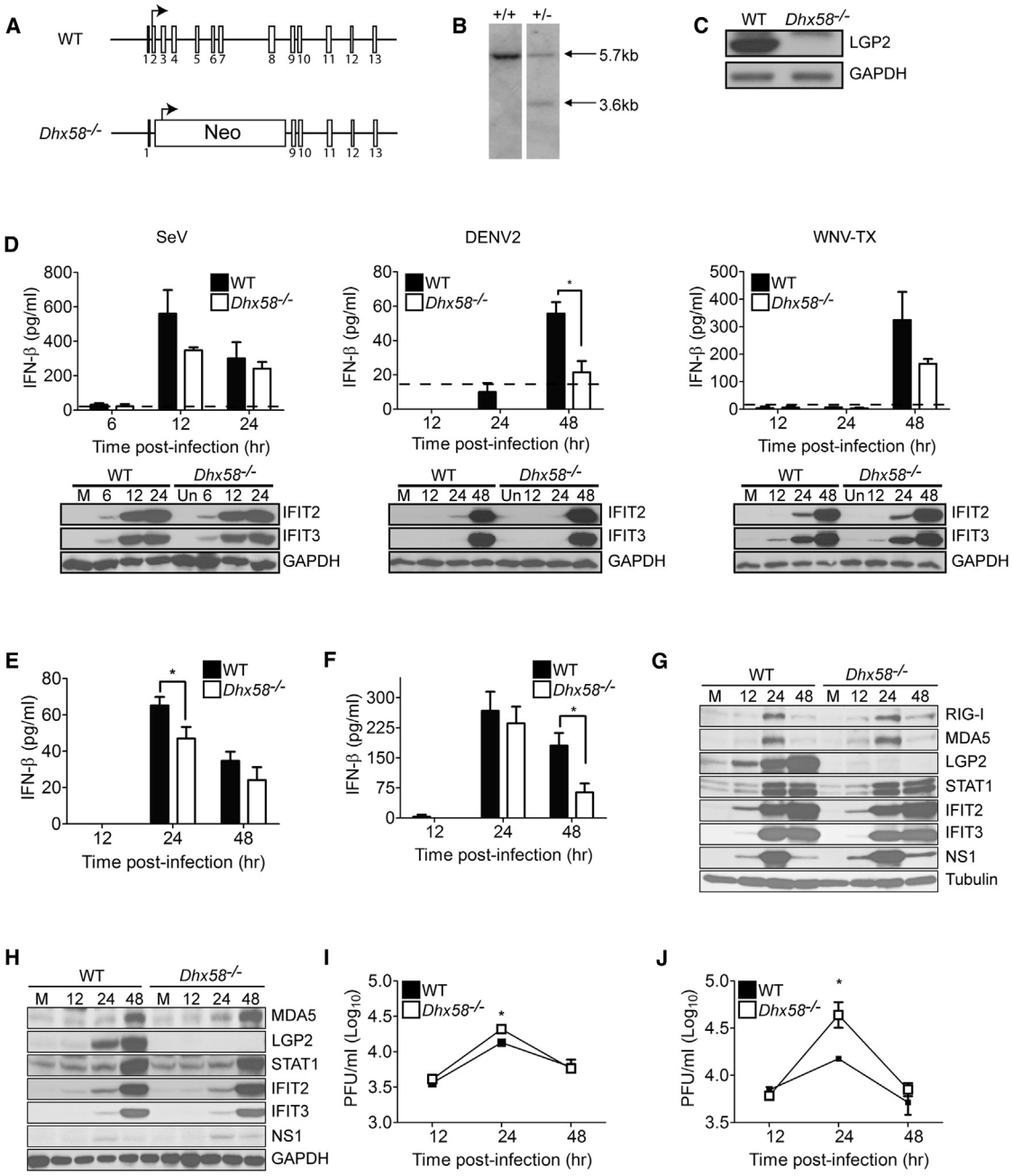

Figure 1. LGP2 Is a Positive Regulator of RLR Signaling in Primary Fibroblasts and Myeloid-Derived Cells

(A) LGP2 gene-targeting strategy and predicted gene disruption.

(B) Southern blot analysis of *Dhx58*$^{+/+}$ and *Dhx58*$^{+/-}$ mice (WT allele = 5.7 kb; *Dhx58*$^{-/-}$ allele = 3.7 kb).

(C) Immunoblot analysis of MEFs from C57BL/6 (WT) and *Dhx58*$^{-/-}$ mice treated with type I IFN for 24 hr.

(D) WT and *Dhx58*$^{-/-}$ MEFs were mock-infected (M) or infected with Sendai virus (200 hemagluttinin units/ml; left panel), DENV-2 (moi 1.0; middle panel), and WNV-TX (moi 1.0; right panel). IFN-β in the supernatant was measured by ELISA (upper) and ISG expression assessed by immunoblotting (lower) at the indicated hr postinfection.

(E–J) Primary bone-marrow-derived DCs and macrophages recovered from WT and *Dhx58*$^{-/-}$ mice were mock infected or infected with WNV-TX at an moi of 1. Cells and culture media were harvested at the times indicated for determination of IFN-β production (E, DCs; F, macrophages), ISG expression (G, DCs; =, H, macrophages), and virus load (I, DCs; J, macrophages).

Dotted lines represent the limit of assay sensitivity. Graphs show the mean ± SD from triplicate samples and representative of three independent experiments. Asterisks denote $p < 0.05$.

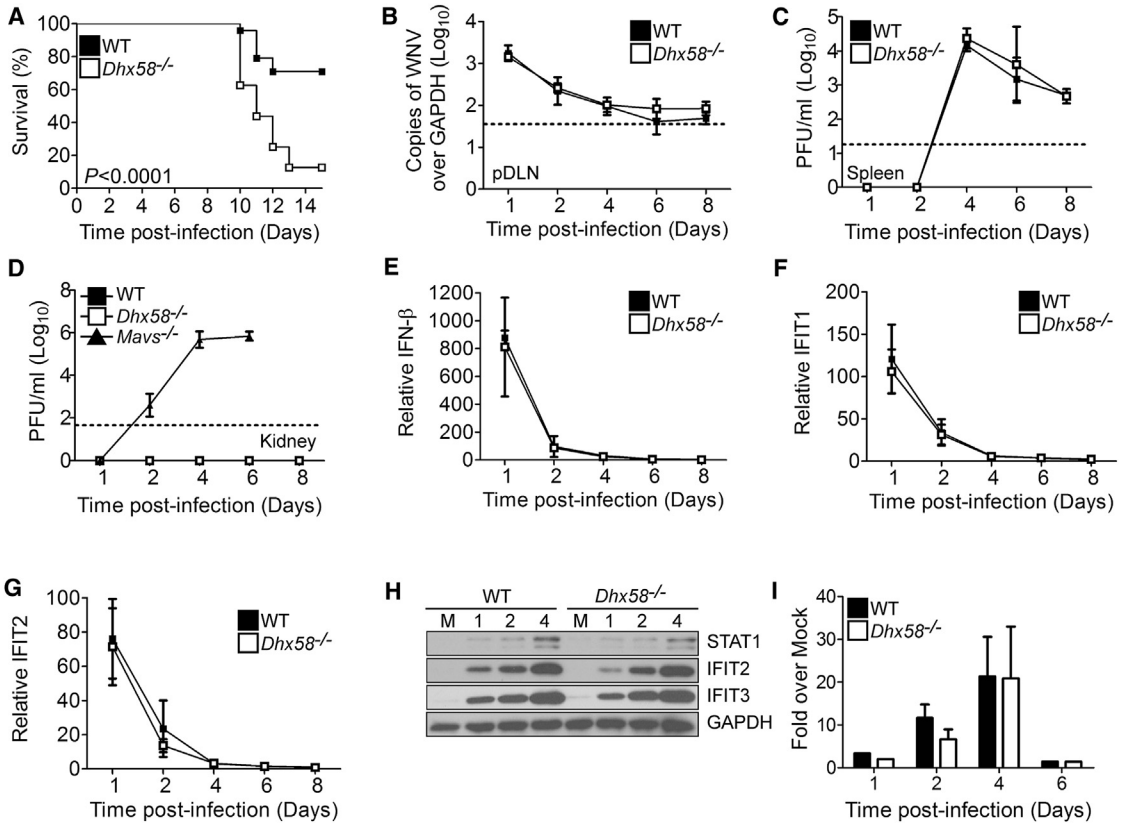

Figure 2. LGP2 Is Required for Protection against WNV Infection

(A) Survival of WT (n = 26) and *Dhx58*$^{-/-}$ (n = 17) adult mice infected s.c. with 100 PFU of WNV-TX.

(B–D) Viral-burden analysis from WT and *Dhx58*$^{-/-}$ infected mice in the (B) pDLN, (C) spleen, and (D) kidney (*Mavs*$^{-/-}$ mice also analyzed).

(E–G) IFN-β (E), IFIT1(F), and IFIT2 expression (G) in the pDLN were determined by qRT-PCR.

(H) Immunoblot analysis of spleens from WT and *Dhx58*$^{-/-}$ mock-infected (M) and WNV-TX-infected mice at the indicated days postinfection.

(I) Serum type I IFN measured by an L929 bioassay.

Dotted lines represent the limit of assay sensitivity. Graphs show the mean ± SD of triplicate biological samples from three independent experiments.

in cortical neurons, as IFN-β induction (Figure 3C) and ISG expression (Figure 3D) were similar between WT and *Dhx58*$^{-/-}$ infected neurons. Although we detected an elevated basal level of STAT1 in *Dhx58*$^{-/-}$ cortical neurons, IFN treatment induced ISG expression similarly between WT and *Dhx58*$^{-/-}$ cells. IFN treatment also induced RLR expression, revealing that RLRs are inducible in neuronal cells. Overall, these results demonstrate that, in neurons, LGP2 does not contribute significantly to regulation of innate immune responses or controlling virus replication.

CNS Inflammation in *Dhx58*$^{-/-}$ Mice during WNV Infection

Because of the absence of a direct effect on viral burden in neurons, we hypothesized that LGP2 might protect against WNV infection in the brain by modulating cell-extrinsic immune control mechanisms. Therefore, we assessed the extent of inflammation and pathology in the brains of WT and *Dhx58*$^{-/-}$ mice after WNV infection. Histological analysis of brain sections recovered from WT mice 8 days after infection revealed moderate inflammation and sparse neuronal damage, consistent with previously published studies (Figure 3E; Suthar et al., 2010).

In addition, mononuclear cell infiltrates were present in the hippocampus and cerebral cortex regions, implying the onset of the inflammatory response that mediates protective immunity to infection. In contrast, brains from *Dhx58*$^{-/-}$ infected mice displayed extensive damage to neurons in the hippocampus and cortex regions, including pyknotic and vacuolated neurons. Surprisingly, we observed little to no inflammation within the hippocampus and cortex of brains from infected *Dhx58*$^{-/-}$ mice, despite the near 3-log increase in brain viral load compared to WT mice. Furthermore, the number of total lymphocytes isolated from the brain of infected *Dhx58*$^{-/-}$ mice was significantly reduced (70% reduction) as compared to WT mice (Figure 3F). Although the brains of infected *Dhx58*$^{-/-}$ mice did not exhibit a significant decrease in the numbers of CD4$^+$ T cells (Figure 3G), there were significantly reduced numbers of total CD8$^+$ T cells (55% reduction; Figure 3H) and antigen-specific CD8$^+$ T cells (62% reduction; Figures 3I and 3J). These results indicate that LGP2 regulates CD8$^+$ T cell recruitment to the CNS.

LGP2 Regulates CD8$^+$ T Cell Accumulation

To define whether the defects in inflammation were specific to the CNS or indicative of a more global inflammatory control

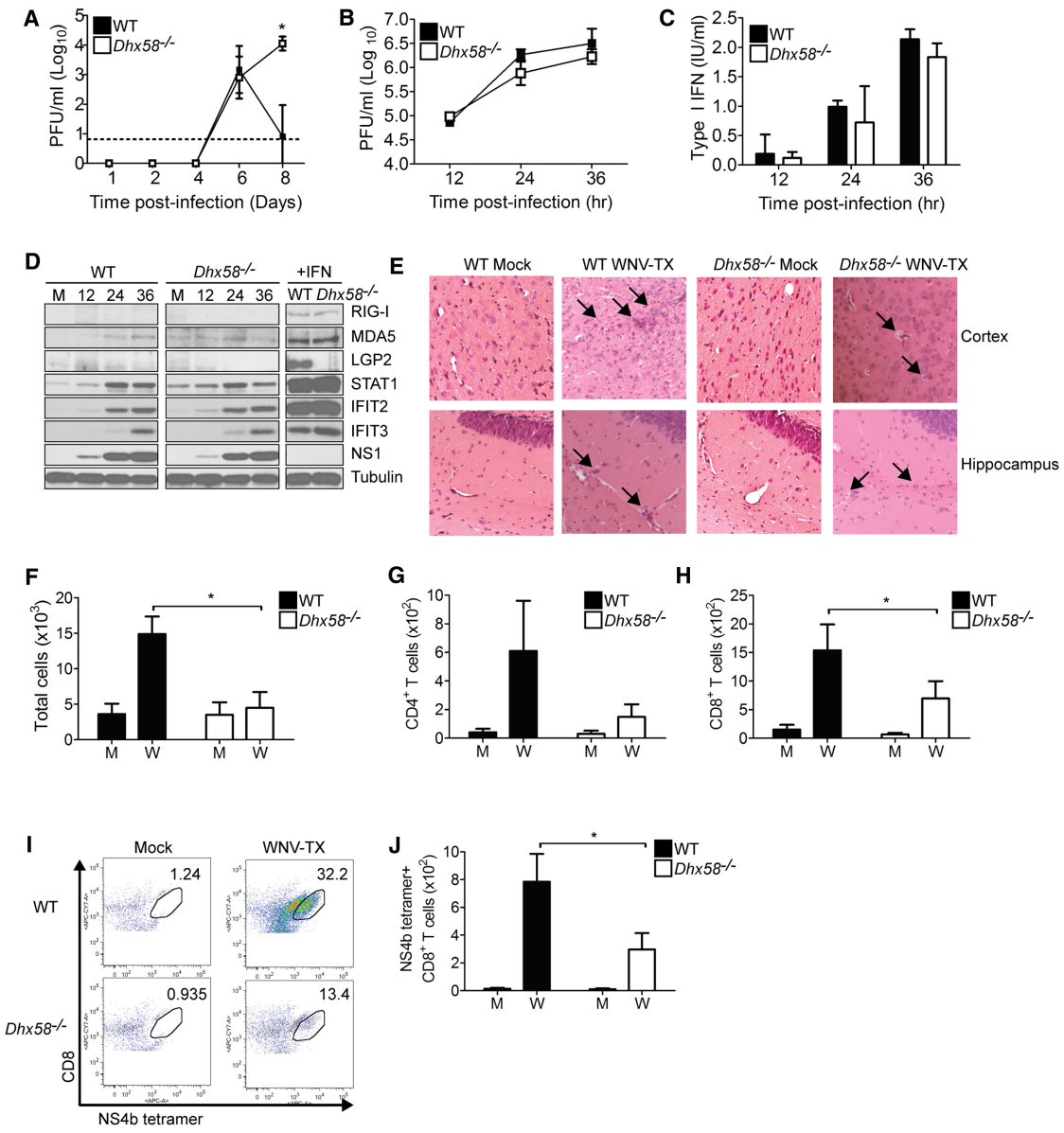

Figure 3. LGP2 Is Required for Regulating CNS Inflammation and Pathology

(A) Viral burden in the brains of infected mice was determined at the indicated days postinfection. The dotted line represents the limit of assay sensitivity.

(B–D) Primary cortical neurons were generated from WT and *Dhx58*$^{-/-}$ mice and infected at an moi of 1, and cell supernatants were collected at the indicated hr postinfection.

(B) Viral titers in the supernatants were determined by plaque assay.

(C) Type I IFN in the supernatants was measured by a bioassay.

(D) Immunoblot analysis from cell lysates of mock (M), WNV-TX-infected, and type I IFN-treated cortical neurons.

(E) H&E-stained sagittal-brain-tissue sections. Arrows denote areas of inflammation and pathology.

(F–J) Brain leukocytes were recovered from WT and *Dhx58*$^{-/-}$ mice eight days postinfection. M, Mock; W, WNV-TX. Graphs show the mean ± SD (n = 3). Data are representative of two or more independent experiments. Asterisks denote $p < 0.05$.

(F) Total cells of brain lymphocytes were determined after cell counting.

(G) Total CD4$^+$ T cells.

(H) Total CD8$^+$ T cells.

(I) Representative flow analysis and gating schematic for identifying NS4b tetramer-specific CD8$^+$ T cells.

(J) Total NS4b tetramer-specific CD8$^+$ T cells.

mechanism of LGP2, we analyzed immune cell composition within the spleens of WNV-infected mice. Spleens recovered from *Dhx58*$^{-/-}$ mice between 4 and 6 days postinfection exhibited similar increases in total lymphocytes to those of spleens from WT infected mice (Figure 4A). However, by day 7 postinfection, spleens from *Dhx58*$^{-/-}$ mice contained significantly lower

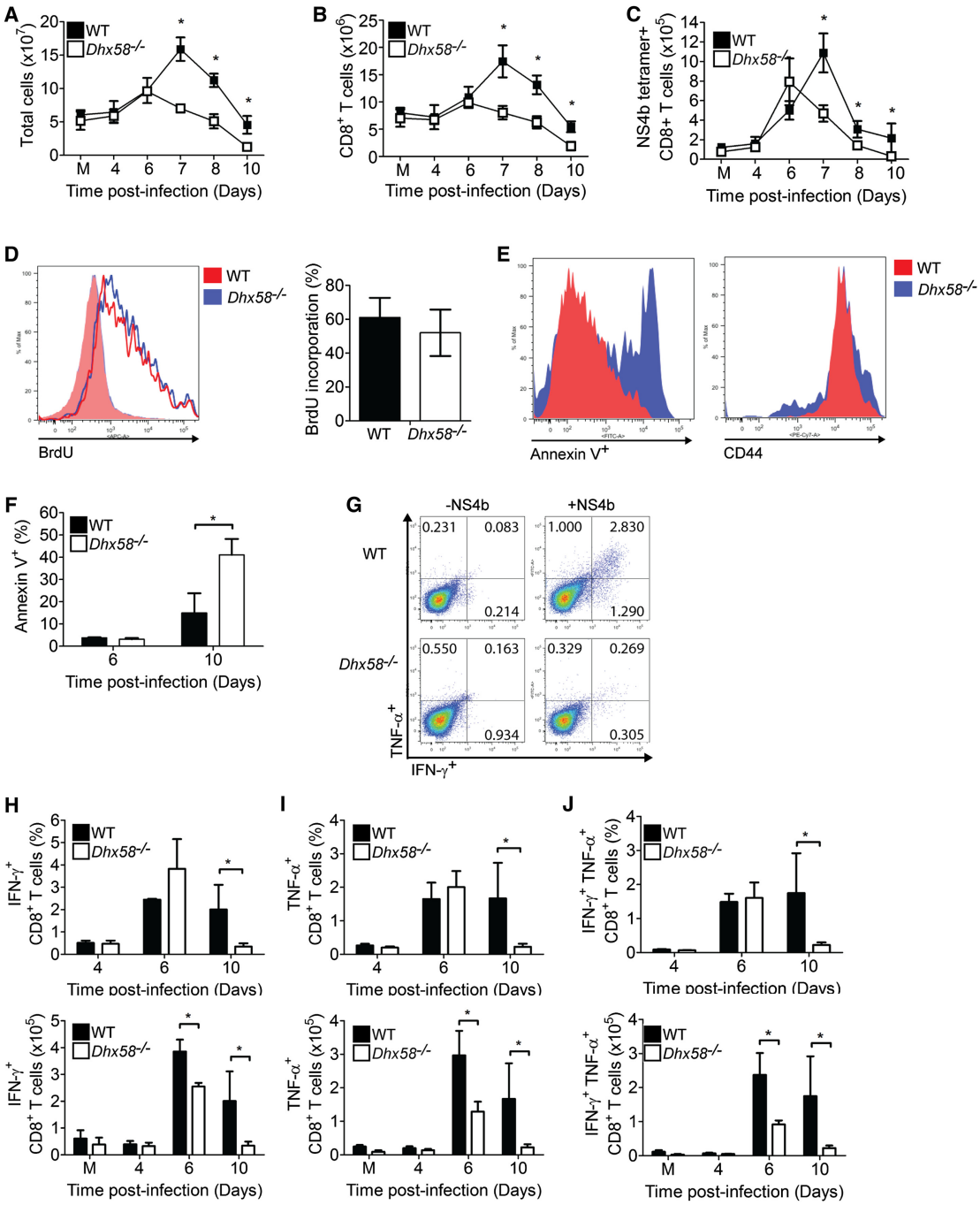

Figure 4. LGP2 Regulates CD8+ T Cell Survival and Fitness

WT and *Dhx58*$^{-/-}$ mice were mock infected (M) or infected with WNV-TX. Spleens were harvested, and immune cells were isolated, counted, and characterized by flow cytometry. Graphs show the mean ± SD from triplicate samples from two or more experiments. Asterisks denote $p < 0.05$.

(A) Total cells (splenocytes).

(B) Total number of CD8+ T cells.

(C) Total number of NS4b tetramer-specific CD8+ T cells.

(D) BrdU incorporation on cells gated on NS4b tetramer-specific CD8+ T cells from day 6 postinfection (left panel, representative histogram; right panel, bar graph).

(E) Annexin V+ (left panel) and CD44 (right panel) staining on NS4b tetramer-specific CD8+ T cells (representative histogram from day 10 postinfection).

(F) Bar graph of Annexin V+ cells.

(G) Flow-cytometry histogram of TNF-α- and IFN-γ-secreting CD8+ T cells upon restimulation with media (left panel) or NS4b peptide (right panel) on day 10 postinfection.

(H–J) Frequency and total number of (H) IFN-γ-, (I) TNF-α-, and (J) IFN-γ- and TNF-α-secreting CD8+ T cells (top panels, frequency; bottom panels, total cells).

total-lymphocyte numbers as compared to spleens from WT infected mice, and this trend continued through day 10 postinfection. We observed similar trends in the number of total CD8+ T cells (Figure 4B) and antigen-specific CD8+ T cells (Figure 4C). Interestingly, and in contrast to mice deficient in RLR signaling (i.e., *Mavs*$^{-/-}$ mice; Suthar et al., 2010), we did not observe differences in either the quantity or the quality of the WNV-specific humoral response (Table S1 available online), suggesting that LGP2 does not directly govern B cell development or CD4+ T cell help during WNV infection (Sitati and Diamond, 2006). Thus, LGP2 modulates CD8+ T cell responses, but not humoral immune responses, against WNV infection.

LGP2 Is Required for CD8+ T Cell Fitness and Survival

To define the mechanisms by which LGP2 regulates CD8+ T cells, we evaluated T cell priming, activation, and expansion in response to virus infection. Ex vivo assessment of bone-marrow-derived DCs and macrophages revealed that the kinetics of maturation of these antigen-presenting cells, as measured by expression of key costimulatory molecules (CD80, CD86, and CD40) and major histocompatibility complex (MHC) classes I and II, were unaltered in the absence of LGP2 (data not shown). Furthermore, in vivo analysis of splenic DCs and macrophages revealed no differences in the expansion or maturation status of each during WNV infection (data not shown), demonstrating that LGP2 does not regulate DC or macrophage maturation. As RLR signaling has been shown to control regulatory T cell expansion during WNV infection (Suthar et al., 2010), we examined this population of cells in WT and *Dhx58*$^{-/-}$ infected mice. In the absence of LGP2, there was no change in regulatory T cell expansion compared to WT infected mice (Figure S1), suggesting that the reduction in CD8+ T cells in *Dhx58*$^{-/-}$ infected mice was not due to aberrant expansion of regulatory T cells during WNV infection.

Because CD8+ T cells are essential for protection against acute WNV infection and the development of WNV encephalitis (Shrestha and Diamond, 2004), and given the robustness of CD8+ T cell responses during WNV infection (Brien et al., 2007, 2008), we assessed the mechanisms by which LGP2 governs CD8+ T cell function. To determine whether LGP2 is required for CD8+ T cell proliferation, WT and *Dhx58*$^{-/-}$ WNV-infected mice were pulsed with bromodeoxyuridine (BrdU) on day 6 postinfection, a time point that directly precedes the dramatic decrease in CD8+ T cell numbers in *Dhx58*$^{-/-}$ infected mice (Figure 4D). Total CD8+ T cells (Figure S2A) and antigen-specific CD8+ T cells from *Dhx58*$^{-/-}$ infected mice showed similar levels of BrdU incorporation to those of WT infected mice, indicating that LGP2 does not regulate CD8+ T cell proliferation. We also assessed a possible role of LGP2 in supporting CD8+ T cell survival after antigen stimulation by analyzing the percentage of CD8+ T cells undergoing apoptosis (as determined by Annexin V+ staining) in WT and *Dhx58*$^{-/-}$ infected mice. On day 6 postinfection, antigen-specific CD8+ T cells from WT and *Dhx58*$^{-/-}$ infected mice showed low but similar frequency of apoptotic cells (Figures 4E and 4F). By day 10 postinfection, antigen-specific (NS4b tetramer+) CD8+ T cells from *Dhx58*$^{-/-}$ infected mice displayed a significant increase (2.7-fold) in apoptotic cell frequency, suggesting that LGP2 regulates CD8+ T cell survival. Similarly, after restimulation with the WNV immunodominant NS4b peptide (Brien et al., 2007; Purtha et al., 2007), splenocytes from *Dhx58*$^{-/-}$ infected mice had reduced frequency and numbers of IFN-γ (Figure 4H), tumor necrosis factor alpha (TNF-α) (Figure 4I), and TNF-α- and IFN-γ-secreting CD8+ T cells (Figure 4J) as compared to WT infected mice, with maximum differences observed on day 10 postinfection. Furthermore, IL-2 expression, an important cytokine for regulating T cell growth and function, was not observed in CD8+ T cells from WT and *Dhx58*$^{-/-}$ mice between days 6 and 10 postinfection (data not shown). To determine whether the reduced numbers of effector T cells in *Dhx58*$^{-/-}$ mice were specific to WNV infection, we evaluated CD8+ T cell survival and fitness after challenge of WT and *Dhx58*$^{-/-}$ mice with another RNA virus, lymphocytic choriomeningitis virus (LCMV)-Armstrong. Similar to that seen after WNV infection, LCMV antigen-specific (GP33 tetramer+) CD8+ T cells from infected *Dhx58*$^{-/-}$ mice showed enhanced apoptosis and reduced effector functions as compared to cells from WT infected mice (Figures S2B and S2C). Together, these results demonstrate that LGP2 participates in the regulation of CD8+ T cell survival and fitness during the immune response to RNA virus infection.

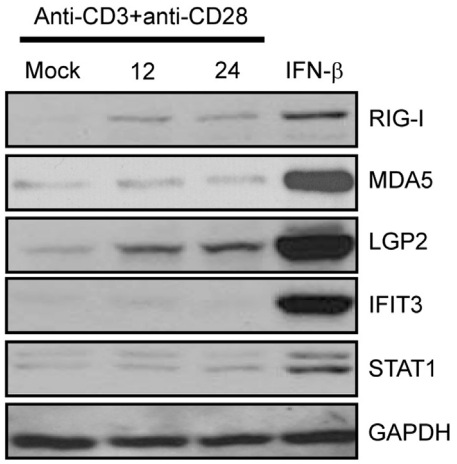

Figure 5. Type I IFN and TCR Conjugation Stimulate Expression of LGP2 and RIG-I in CD8+ T Cells

CD8+ T cells were purified from WT mice through negative selection and stimulated with plate-bound anti-CD3 and anti-CD28. Parallel cultures were treated with IFN-β (100 IU/ml) for 24 hr. Cell lysates were collected and immunoblot analysis was performed using the indicated antibodies. Data are representative of three independent experiments.

LGP2 Is Expressed in CD8+ T Cells and Regulates Survival in a Cell-Intrinsic Manner

We next measured RLR expression and abundance in purified CD8+ T cells recovered from WT mice. In general, CD8+ T cells expressed a low basal level of each RLR, including LGP2, and RLR abundance increased along with other ISGs when the cells were treated with IFN-β (Figure 5). Stimulation of CD8+ T cells with plate-bound anti-CD3 and anti-CD28 induced RLR expression, with LGP2 expression accumulating to the highest levels among the RLRs (Figure 5). These findings demonstrate that LGP2 expression in CD8+ T cells is induced by type I IFN and TCR signaling, suggesting a cell-intrinsic role for LGP2 in regulation of CD8+ T cell fitness during RNA virus infection.

To establish whether LGP2 functions in a cell-intrinsic or cell-extrinsic manner to promote CD8+ T cell survival, we isolated CD8+ T cells from CD45.1 congenic WT mice and *Dhx58*$^{-/-}$ (CD45.2) mice and adoptively transferred them into *Rag1*$^{-/-}$ mice at a 1:1 cell ratio. One day after transfer, recipient mice were injected with diluent alone (uninfected control) or challenged with WNV (Figure 6A). Examination of donor cells in uninfected *Rag1*$^{-/-}$ recipient mice showed comparable division of carboxyfluorescein succinimidyl ester (CFSE)-labeled WT and *Dhx58*$^{-/-}$ CD8+ T cells (Figure 6B), with low Annexin V+ staining apparent in either WT- or *Dhx58*$^{-/-}$-derived CD8+ T cells (data not shown). Thus, in the absence of infection, *Dhx58*$^{-/-}$ CD8+ T cells do not show overt defects in homeostatic proliferation or survival. However, the frequency and total numbers of antigen-specific *Dhx58*$^{-/-}$CD8+ T cells were reduced by day 8 post-WNV-infection (Figure 6C). To determine whether this reduction was due to turnover of cells or an inability of cells to effectively proliferate, we evaluated BrdU incorporation on day 8 postinfection. Antigen-specific *Dhx58*$^{-/-}$ CD8+ T cells displayed enhanced proliferation as compared to WT CD8+ T cells (Figure 6D), demonstrating that dysregulated cell proliferation does not account for the reduction in CD8+ T cells. Another possible explanation for the reduction in CD8+ T cells is dysregulated development of short-lived effector cell (SLEC) and memory-precursor effector cell (MPEC) populations in the absence of LGP2 (Joshi et al., 2007). Antigen-specific *Dhx58*$^{-/-}$ CD8+ T cells displayed comparable percentages of KLRG1-expressing cells, a marker for discriminating SLECs, and IL-7Rα (CD127)-expressing cells, a marker for discriminating MPECs (Figure S3). This suggests that LGP2 is not required for programming development of SLEC or MPEC populations during WNV infection. Consistent with our previous observations, antigen-specific *Dhx58*$^{-/-}$CD8+ T cells displayed increased Annexin V+ staining compared to WT CD8+ T cells (Figure 6E). Furthermore, when restimulated with the immunodominant NS4b peptide ex vivo (Figure 6F), CD8+ T cells from *Dhx58*$^{-/-}$ mice exhibited compromised effector functions compared to WT cells, including a reduction in single-positive IFN-γ- (41.5% reduction; $p = 0.001$), TNF-α- (40.5% reduction; $p = 0.004$), and double-positive TNFα- and IFN-γ-secreting cells (43.9% reduction; $p = 0.004$).

LGP2 has been reported to bind to MAVS to regulate RLR signaling (Komuro and Horvath, 2006). Therefore, we assessed the role of MAVS in regulating CD8+ T cell survival using the adoptive transfer model. We observed no enhancement of cell death in *Mavs*$^{-/-}$ CD8+ T cells (data not shown), consistent with our previous studies (Suthar et al., 2010). Taken together, these results demonstrate that LGP2 functions in a cell-intrinsic manner to promote CD8+ cell survival and function after antigen stimulation, independently of MAVS.

LGP2 Imparts Sensitivity to CD95-Mediated Cell Death

Cell death in T cells can occur through activation of the intrinsic apoptosis pathway, involving Bcl-2, Bim, and Bcl-xL, or through the extrinsic pathway, initiated by death-receptor signaling (Tourneur and Chiocchia, 2010). Using the adoptive transfer model, we evaluated key components in the intrinsic and extrinsic apoptosis signaling pathways to identify the mechanism by which LGP2 operates to control CD8+ T cell survival. In the absence of LGP2, antiapoptotic factors, including Bcl-2 and Bcl-xL, and the proapoptotic factor Bim displayed expression in antigen-specific CD8+ T cells similar to that of WT CD8+ T cells, suggesting that LGP2 does not regulate the intrinsic apoptosis signaling pathway through altered expression of these factors (Figure S4). In contrast, antigen-specific *Dhx58*$^{-/-}$ CD8+ T cells displayed enhanced caspase-8 (Figure 7A) and caspase-3 and -7 activity (Figure 7B), suggesting that LGP2 regulates the extrinsic apoptosis signaling pathway. Members of the TNF superfamily are important for regulation of the extrinsic apoptosis pathway in T cells. For example, ligation of TNFα, TNF-related apoptosis-inducing ligand (TRAIL), and CD95 ligand (CD95L) to their cognate receptors (TNF-RI and -RII, TRAIL-R2, and CD95, respectively) leads to formation of the death-inducing signaling complex followed by activation of caspase-8, activation of caspase-3 and caspase-7, and ultimately cell death (Aggarwal, 2003). In the absence of LGP2, antigen-specific CD8+ T cells displayed enhanced expression of TNF-RI (Figure 7C), TNF-RII (Figure 7D), TRAIL-R2 (Figure 7E), and CD95 (Figure 7F) compared to WT CD8+ T cells during virus infection. To determine whether the enhanced receptor expression correlated with increased sensitivity to cell death, splenocytes were treated exogenously with TNF-α, TRAIL, or CD95L, and cell death was evaluated in antigen-specific CD8+ T cells. Consistent with ex vivo examination (Figure 6E), antigen-specific CD8+ T cells from *Dhx58*$^{-/-}$ mice displayed enhanced Annexin V+ staining as compared to WT cells in the absence of exogenous treatment, further demonstrating an overall increased sensitivity for cell death in the absence of LGP2 (Figures 7G–7I). WT or *Dhx58*$^{-/-}$ antigen-specific CD8+ T cells displayed no enhancement of cell death upon treatment with TNF-α (Figure 7G), whereas treatment with TRAIL led to similar increases in cell death between WT and *Dhx58*$^{-/-}$ antigen-specific CD8+ T cells (Figure 7H). In contrast, treatment with CD95L led to an increase in cell death of antigen-specific CD8+ T cells from *Dhx58*$^{-/-}$, but not WT mice (Figure 7I). In fact, CD95L-treated *Dhx58*$^{-/-}$ CD8+ T cells displayed an increase in cell death from 21% to 32.5% upon ex vivo treatment as compared to WT CD8+ T cells (7.8% Annexin V+ cells in treated and untreated conditions). Although we did not observe a similar enhancement of sensitivity over WT CD8+ T cells upon TNF-α or TRAIL treatment, we cannot preclude the possibility that signaling through these pathways or other death receptors within the TNF superfamily contributes to the enhanced death of antigen-specific *Dhx58*$^{-/-}$ CD8+ T cells during virus infection. Taken together, these findings demonstrate a role for LGP2 in promoting CD8+ T cell survival through regulation of sensitivity to death-receptor-mediated signaling of cell death.

DISCUSSION

Our study defines an essential role for LGP2 in promoting immunity through cell-intrinsic regulation of CD8+ T cell survival and fitness. We found that LGP2 promotes CD8+ T cell survival by controlling sensitivity to death-receptor signaling. This finding is highly relevant to the outcome of WNV infection because CD8+ T cells are the critical immune cell that controls virus replication and spread within the CNS (Shrestha and Diamond, 2004). In the absence of LGP2, CD8+ T cells did not continue to expand to WT levels during viral infection, but instead

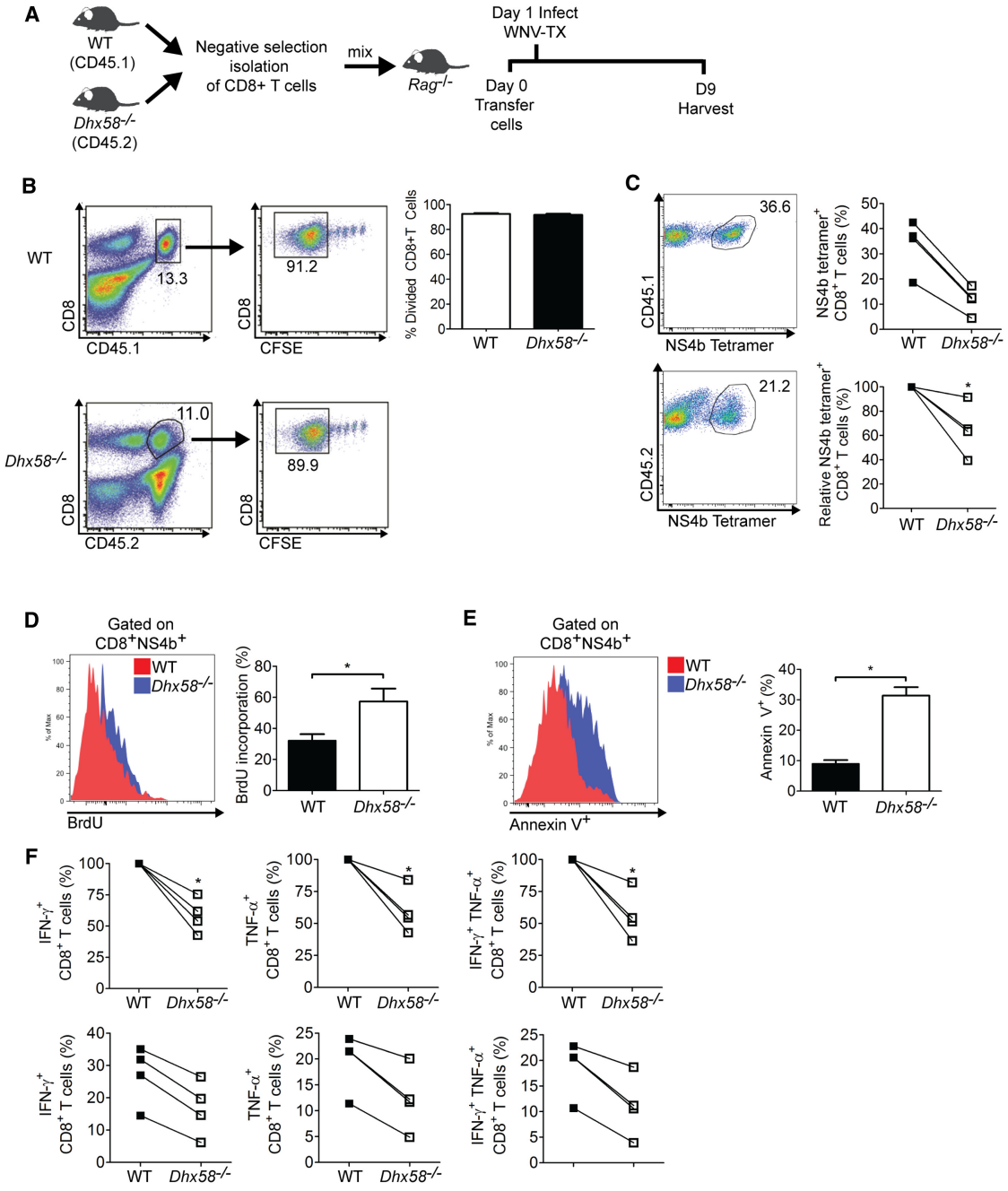

Figure 6. LGP2 Directly Regulates CD8+ T Cell Survival and Fitness

(A) Schematic of CD8+ T cell adoptive transfer into *Rag1*$^{-/-}$ mice.

(B) Homeostatic proliferation of CD8+ T cells from WT (CD45.1) and *Dhx58*$^{-/-}$ (CD45.2) measured by flow cytometry (left panels, representative flow-cytometry analysis and gating schematic; right panel, bar graph displaying frequency of divided CD8+ T cells).

(C) NS4b tetramer-specific CD8+ T cells from day 8 postinfection (each connecting line represents cells isolated from the same *Rag1*$^{-/-}$ recipient host; top right panel, frequency; bottom right panel, relative ratio of NS4b tetramer+CD8+ T cells).

(D) BrdU staining of NS4b tetramer-specific CD8+ T cells from WNV-TX-infected mice on day 8 postinfection (representative flow analysis and bar graph displaying frequency of BrdU+ staining).

(E) Annexin V+ staining of NS4b tetramer-specific CD8+ T cells (representative flow analysis and bar graph displaying frequency of Annexin V+ staining).

(F) Total number of WNV-specific CD8+ T cells secreting IFN-γ (left panels), TNF-α (middle panels), or both (right panels). Relative to WT (top panels) and actual (bottom panels) percentages of CD8+ T cells isolated from the same *Rag1*$^{-/-}$ recipient host.

Graphs show the mean ± SD (n = 3), and data are representative of two or more independent experiments. Asterisks denote $p < 0.05$.

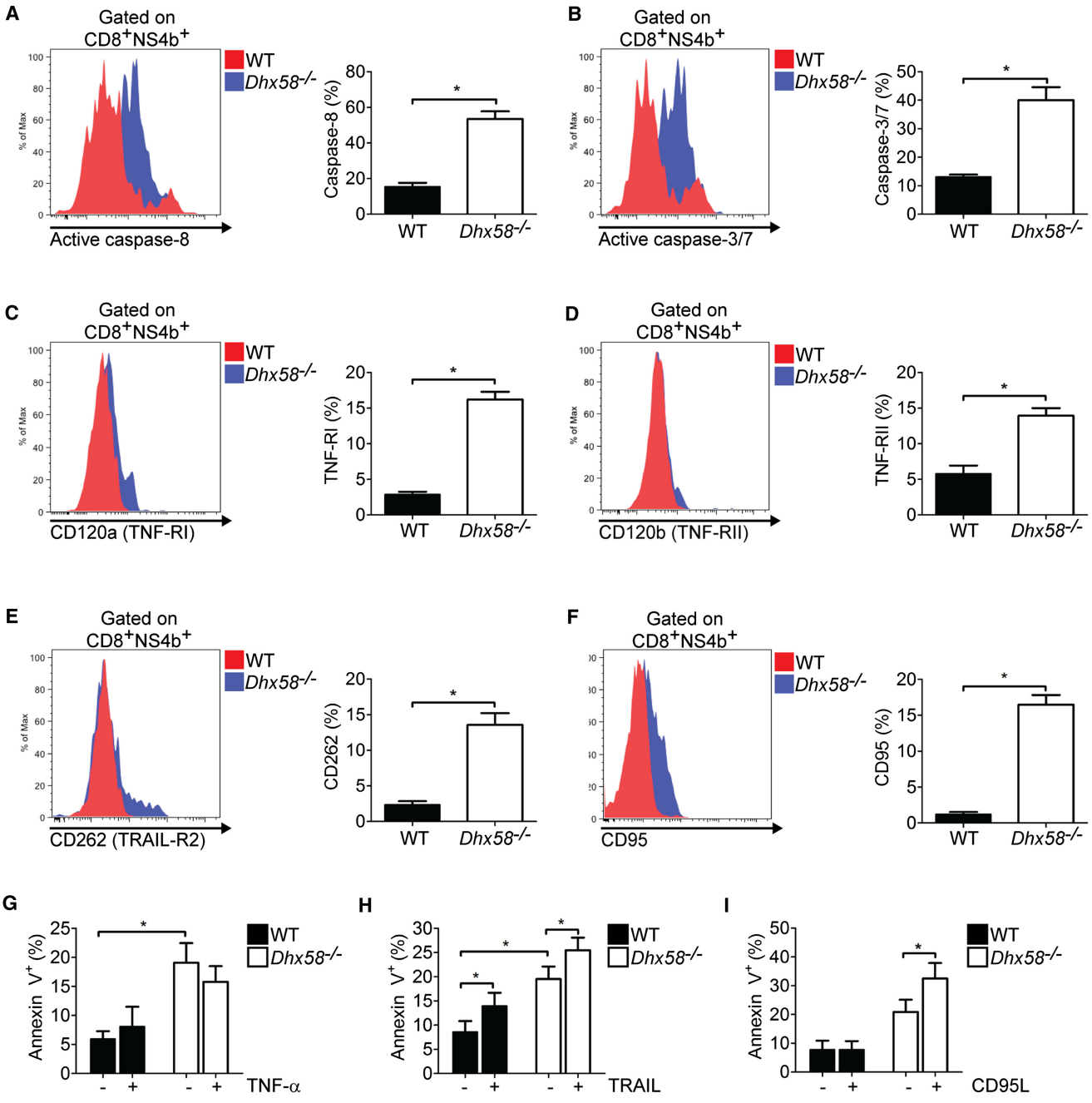

Figure 7. LGP2 Controls Sensitivity to CD95-Mediated Apoptosis Signaling

(A–F) Active caspase-8 (A), active caspase-3 and -7 (B), CD120a (C), CD120b (D), CD262 (E), and CD95 (F) expression measured on NS4b tetramer-specific CD8+ T cells from WNV-TX-infected mice on day 8 postinfection (representative flow analysis and bar graph displaying frequency of positive staining).

(G–I) Sensitivity to cell death upon ex vivo treatment with (G) TNF-α, (H) TRAIL, or (I) CD95 ligand.

Splenocytes from adoptively transferred *Rag1*$^{-/-}$ infected mice were isolated and treated on day 8 postinfection. Graphs show the mean ± SD (n = 3), and data are representative of two independent experiments. Asterisks denote $p < 0.05$.

displayed increased cell death concomitant with decreased effector function. Furthermore, using an adoptive transfer system, we demonstrated that LGP2 acts in a T cell-intrinsic manner to mediate a prosurvival response. Although we found that LGP2 functions in activated CD8+ T cells independent of canonical MAVS signaling of RLRs, it remains possible that it may interact with either RIG-I or MDA5 to regulate prosurvival functions of T cells. Together, these findings reveal a role for LGP2 in CD8+ T cell-mediated immunity to viral infection, and assigns an essential role for LGP2 in programming antigen-induced survival.

LGP2 has been described as both a positive and negative regulator of RLR signaling of innate immune defenses against

RNA viruses in vitro (Komuro and Horvath, 2006; Rothenfusser et al., 2005; Saito et al., 2007) and has been proposed to enhance signaling induced by RIG-I or MDA5 in vivo (Satoh et al., 2010). Our analyses of *Dhx58*$^{-/-}$ primary cells ex vivo validate a positive, albeit cell-specific, role for LGP2 in RLR signaling of innate defenses, in that LGP2 contributed to sustained RLR signaling of IFN-β expression. In the absence of LGP2, IFN-β production from myeloid cells, but not MEFs, was reduced in response to RNA virus infection, including WNV and DENV2, two flaviviruses that trigger innate immune defenses through a combination of RIG-I and MDA5 actions (Fredericksen et al., 2008; Loo et al., 2008). However, our studies also showed that LGP2 is not essential for RLR signaling of innate antiviral defenses. These findings contrast with a previous report that concluded that LGP2 was essential for RLR signaling of innate immunity (Satoh et al., 2010). These differences can probably be attributed to differences in the genetic background of the mutant mice and gene-targeting strategies between each study. Importantly, our studies utilized a *Dhx58*$^{-/-}$ mouse that was generated directly on a pure C57BL/6 background and through the complete disruption of LGP2 transcription, differing from prior *Dhx58*$^{-/-}$ mouse lines, which exist in mixed genetic backgrounds and were created with gene-targeting approaches that retained the transcriptional start site to render possible messenger RNA expression from the targeted gene (Satoh et al., 2010; Venkataraman et al., 2007). Although our data overall support a role for LGP2 as a positive cofactor of innate immune signaling, it remains possible that, under certain conditions, LGP2 also may function to suppress RLR signaling, in that high LGP2 expression was shown to mediate RLR signaling suppression in several independent studies (Komuro and Horvath, 2006; Rothenfusser et al., 2005; Saito et al., 2007; Venkataraman et al., 2007; Yoneyama et al., 2005). Additional studies under conditions of regulated LGP2 expression in vivo are required to fully ascertain its role in RLR signaling control.

During virus infection or antigen stimulation, CD8$^+$ T cells receive multiple signals to undergo rapid proliferation and maintain survival. Both cell-intrinsic and -extrinsic apoptotic signaling pathways are important in regulating peripheral deletion of activated CD8$^+$ T cells (Michalek and Rathmell, 2010). During the expansion phase, expression of pro- and antiapoptotic Bcl-2 family members is suppressed, and it remains low through the cell contraction or death phase, wherein dysregulation of these processes can lead to premature T cell death (Grayson et al., 2000). In the absence of LGP2, however, we observed comparable expression of Bcl-2 family members during virus infection, suggesting that LGP2 does not impart regulation of the intrinsic apoptosis signaling pathway that is linked with altered expression of Bcl-2 family proteins. Among programs controlling effector T cell contraction, the cell-extrinsic apoptosis pathway is critical for peripheral deletion of activated CD8$^+$ T cells through death-receptor signaling (Zhang et al., 2005). In particular, CD95 signaling and, to a lesser degree, TNF-α signaling play important roles in maintaining CD8$^+$ T cell homeostasis and shaping the peripheral T cell repertoire during infection. In contrast, "helpless" CD8$^+$ T cells undergo TRAIL-mediated cell death upon reactivation during a secondary challenge (Janssen et al., 2005). Under our experimental conditions, we observed enhanced expression of death receptors in antigen-specific *Dhx58*$^{-/-}$ CD8$^+$ T cells, suggesting that LGP2 is important in controlling receptor expression and, hence, sensitivity to death-receptor-mediated cell death. Using an ex vivo model, we determined that the absence of LGP2 led to enhanced sensitivity to CD95-mediated cell death, but not to TNF-α or TRAIL treatment as compared to WT treated cells. A lack of TNF-α or TRAIL enhancement of cell death in *Dhx58*$^{-/-}$ cells does not preclude the possibility that these death receptors contribute to the enhanced cell death that is observed in antigen-specific *Dhx58*$^{-/-}$ CD8$^+$ T cells. Overall, our observations imply that LGP2 functions as a molecular switch to control (by preventing or limiting) death-receptor signaling during the early stages of T cell activation. We propose three unique mechanisms by which cell death could be regulated by LGP2: (1) signaling initiated by protein or RNA interactions of LGP2 imparts LGP2 actions that regulate prosurvival or proapoptotic factor(s); (2) LGP2 signals the expression of prosurvival or apoptotic gene expression in response to the binding of specific inducer RNA(s); or (3) LGP2 regulates the synthesis of prosurvival microRNA species in antigen-stimulated T cells. Despite comparably low levels of RIG-I or MDA5 expression upon T cell receptor (TCR) conjugation, it is remains plausible that LGP2 could also work in conjunction with the other RLRs to promote CD8$^+$ T cell survival. Due to the embryonic lethality of RIG-I-deficient mice in a pure C57BL/6 background, we are unable to evaluate the role of RIG-I in CD8$^+$ T cells at this time (Kato et al., 2006). However, we and others have evaluated WNV infection in MDA5-deficient mice and observed normal proliferation and survival of antigen-specific CD8$^+$ T cells (data not shown), consistent with a lack of induction of MDA5 expression upon TCR conjugation. These observations suggest that LGP2 functions independently of MDA5 to govern CD8$^+$ T cell survival during virus infection. In support of the third possibility, recent work has shown that the RNAi pathway protein Dicer, which regulates microRNA biogenesis, is required for mediating CD8$^+$ T cell survival, proliferation, and effector functions (Zhang and Bevan, 2010), and it has recently been demonstrated that LGP2 can directly interact with components of the RNAi biogenesis pathway, including Dicer and Argonaut2 (Li et al., 2011). In addition, evolutionary studies have suggested that the RLRs and Dicer have evolved through a common ancestor, suggesting commonalities in function (Sarkar et al., 2008; Zou et al., 2009). Thus, it is reasonable to speculate that LGP2 promotes T cell survival and fitness by regulating gene expression through governance of microRNA expression. These possibilities are currently under investigation.

The production of type I IFN and subsequent innate immune responses is a key linkage point between innate and adaptive immunity, specifically during T cell function (Havenar-Daughton et al., 2006; Kolumam et al., 2005; Thompson et al., 2006). Both TCR stimulation and type I IFN treatment induced RLR expression in T cells. Though there is little overlap in type I IFN and TCR signaling pathways, these findings strongly suggest that each may converge on a common transcriptional element that regulates the expression of LGP2 and the other RLRs.

In addition to LGP2, the Toll-like receptor adaptor molecule MyD88 functions in a cell-intrinsic manner to support CD8$^+$ and CD4$^+$ T cell survival (Gelman et al., 2004; Quigley et al., 2009; Rahman et al., 2008; Zhao et al., 2009). Although we observed little requirement for LGP2 in the CD4$^+$ T cell response after WNV or

LCMV infection, it is possible that LGP2 or other RLRs may be required for CD4+ T cell response during infection by other viruses or intracellular pathogens. Consistent with this, MAVS provides an important signal that controls regulatory T cell expansion during viral infection (Suthar et al., 2010). Thus, RLRs and TLRs probably have a prominent role in coordinating signals that regulate priming and/or survival of T cell responses during viral infection.

Overall, our results reveal a role for LGP2 in the survival of activated CD8+ T cells during virus infection. Cell-mediated responses are essential for protection and clearance of many virus infections and are critical for successful vaccines against many pathogens (Pulendran and Ahmed, 2011). Thus, our findings have direct implications for vaccine and adjuvant design strategies aimed at eliciting sustained antiviral T cell-mediated responses. Drug designs that engage LGP2 or its downstream signaling pathways could enhance T cell survival and effector function for the control of virus infection or, alternatively, promote cell death for the limitation of immune-mediated pathology.

EXPERIMENTAL PROCEDURES

Cells and Viruses

BHK-21, L929, and L929-ISRE reporter (kind gift from B. Beutler) cells were cultured in Dulbecco's modified Eagle's medium supplemented with 10% fetal bovine serum (FBS), HEPES, L-glutamine, sodium pyruvate, antibiotic-antimycotic solution, and nonessential amino acids. WNV isolate TX 2002-HC (WNV-TX) was described previously (Keller et al., 2006) and titered with a standard plaque assay on BHK-21 cells. Working stocks of WNV-TX were generated by as previously described (Suthar et al., 2010). LCMV (Armstrong strain) was plaque purified, grown in BHK-21 cells, and titered as previously described (Thompson et al., 2006). DENV2 was a gift from J. A. Nelson (Oregon Health and Sciences University). Sendai virus (SeV) strain Cantell was obtained from the Charles River Laboratory.

Generation of LGP2-Deficient Mice

A conventional mouse LGP2 gene (encoded by *Dhx58*) deletion procedure was performed by inGenious Targeting Laboratory (Stonybrook, NY, USA). The targeting vector was subcloned from a positively identified C57BL/6 Bacterial Artifical Chromosome (BAC) clone using a homologous recombination-based technique. The 13.9kb region that was subcloned contains exons 2–8 of DHX58. The long homology arm is located on the 5′ side of exon 2 and is 7.57 kb long, and the short homology arm extends 1.46 kb 3′ to exon 8. A neomycin positive-selection cassette flanked by *loxP* sites replaced 4.8 kb of the gene including exon 2–8 and the ATG start codon in exon 2. A NotI-linearized targeting construct was transfected into iTL IC1 C57BL/6 embryonic stem cells after electroporation. After selection in G418 antibiotic, surviving clones were expanded for PCR analysis to identify recombinant embryonic stem cell clones. The correctly targeted embryonic stem cell clones were microinjected into C57BL/6J blastocysts. The resulting chimeric mouse was mated with a WT C57BL/6J mouse to establish germlime transmission. The heterozygous mice (F1 mice) were interbred to obtain homozygous *Dhx58*$^{-/-}$ mice. The genotypes of the mice were determined by Southern blot analysis (genomic DNA was cut with PvuII; 543 bp primer probe was generated by the following primers: WPB1 5′-GAAGTCCCTTCTGGGTCCGGGTAC-3′; WPB2 5′-ATTCT CCCTAGCCTACTGAGTGAC-3′; and PCR (primers: F7, 5′–GGAACTTCGCTA GACTAGTACGCGTG-3′; A6, 5′-GACAGGACTTGGACATGGACACC-3′).

Mouse Experiments

Sti$^{-/-}$ mice (C57BL/6 background; referred to in text as *Mavs*$^{-/-}$) were generated in the Gale laboratory in a manner similar to the *Dhx58*$^{-/-}$ mice described in the previous section. The generation and characterization will be discussed in a future publication. C57BL/6 WT inbred mice, CD45.1 mice, and *Rag1*$^{-/-}$ mice were commercially obtained (Jackson Laboratories, Bar Harbor, ME, USA). All mice were genotyped and bred in specific pathogen-free conditions in the animal facility at the University of Washington. Experiments were performed in accordance with the University of Washington Institutional Animal Care and Use Committee guidelines. Age-matched 6- to 12-week-old mice were inoculated subcutaneously (s.c.) in the left rear footpad with 100 plaque-forming units (PFUs) of WNV-TX in a 10 μl inoculum diluted in Hank's balanced salt solution supplemented with 1% heat-inactivated FBS. Mice were monitored daily for morbidity and mortality. A total of 2 × 10^5 PFU of LCMV was injected via an intraperitoneal route.

Adoptive Transfers

CD8+ T cells were isolated directly from CD45.1 and *Dhx58*$^{-/-}$ splenocytes using the negative selection CD8+ T Cell Isolation Kit (Miltenyi Biotec) according to the manufacturer's instructions (greater than 90% purity). Purified CD8+ T cells (2 ×10^6 for each mouse strain) were resuspended in cold PBS and mixed 1:1 in a total volume of 100 μl. Cells were transferred into sex-matched *Rag1*$^{-/-}$ mice by intravenous injection through the tail vein. The following day (24 hr posttransfer), mice were infected with 100 PFU WNV-TX through the s.c. route in the left rear footpad, and mice were monitored daily as described in the previous section.

Viral Tissue Burden and Quantification

For in vivo studies, infected mice were euthanized, bled, and perfused with 20 ml of PBS. The whole brain, kidney, and spleen were removed, weighed, and homogenized in 500 μl of PBS containing 1% heat-inactivated FBS, using a Precellys 24 at 1,500 rpm for 20 seconds (Bertin Technologies, France). Sample homogenates were titered by plaque assay on BHK cells. For analysis of the viral load within the DLN, the pDLN was harvested and total RNA was extracted (using the RNeasy Kit [Qiagen]), DNase treated (Ambion), and WNV RNA copy number was measured by qRT-PCR as previously described (Suthar et al., 2010).

Primary Cell Isolation and Infection

Bone-marrow-derived DCs and macrophages were generated as described previously (Daffis et al., 2008). The DCs or macrophages were infected with WNV-TX at an multiplicity of infection (moi) of 1. At the indicated time points, supernatants were collected for evaluating viral titers and IFN-β by ELISA. Cells were collected in parallel for immunoblot analysis. Cortical neurons were isolated from 15-day-old embryonic mice and cultured as described previously (Samuel et al., 2006). On day 6 of the culture, neurons were infected with WNV-TX at an moi of 1, supernatants were collected for virus titration, and cells were collected for RNA analysis by qRT-PCR using primers described previously(Suthar et al., 2010).

Immunoblot Analysis

Cells were lysed in radioimmunoprecipitation assay buffer containing a cocktail of protease and phosphatase inhibitors (Sigma-Aldrich). Protein extracts (25 μg) were analyzed by immunoblotting as described previously (Suthar et al., 2010). The following primary antibodies were used to probe blots: mouse anti-WNV from the Center for Disease Control; rabbit anti-ISG54 and rabbit anti-ISG49, kindly provided by G. Sen; rabbit anti-MDA5 from Immuno-Biological Laboratories; mouse anti-tubulin from Sigma-Aldrich; rabbit anti-GAPDH from Santa Cruz Biotechnology; rabbit anti-STAT1 from Cell Signaling; and rabbit anti-RIG-I, generated as previously described (Loo et al., 2008). Secondary antibodies (peroxidase-conjugated goat anti-rabbit, goat anti-mouse, donkey anti-rabbit, and donkey anti-mouse) were from Jackson ImmunoResearch.

RNA Extraction and Analysis

For cultured cells, total RNA was extracted using the RNeasy Kit (Qiagen), DNase treated (Ambion), and evaluated for ISG49, ISG54, and IFN-β RNA expression by SYBR Green qRT-PCR. Specific primer sets for ISG-49, ISG-54, and IFN-β have been described previously (Suthar et al., 2010).

Interferon Bioassay and ELISA

IFN-α and -β were measured in sera using a biological assay as previously described (Suthar et al., 2010). IFN-β in cell culture supernatants was analyzed using mouse-specific ELISA kits from PBL Biomedical Laboratories according to the manufacturer's protocol. One hundred μl from mock-infected and WNV-TX-infected neuronal supernatant was used to treat L929-ISRE reporter cells, and luciferase units were measured 6 hr posttreatment.

WNV-Specific Antibody Analysis

WNV-specific immunoglobulin M and G (IgM and IgG) levels were determined with an ELISA using purified recombinant E protein as previously described (Shrestha et al., 2006). The neutralization titer of serum antibody was determined by using a previously described plaque-reduction neutralization assay (Diamond et al., 2003a). The dilution at which 50% of plaques were neutralized was determined after nonlinear transformation of the data.

Histological Analysis

Mock-infected or WNV-infected mice were perfused with PBS (4% paraformaldehyde, pH 7.3). Brains were embedded in paraffin, and 10 μm sections were prepared and stained with hematoxylin and eosin (H&E) by the University of Washington Pathology Histology Laboratory. Sections were analyzed using a Nikon Eclipse E600 microscope (University of Washington Keck Microscope Facility).

Flow-Cytometric Analysis

Splenocytes were isolated, washed, and resuspended in complete RPMI 1640 media (containing 10% FBS), L-glutamine, and antibiotic-antimycotic solution (cRPMI) before in vitro stimulation. Cells were washed twice before flow-cytometry staining. For isolation of CNS immune cells, mice were euthanized and perfused extensively with PBS to remove residual intravascular leukocytes. Brains were isolated and minced in RPMI media, triturated, and digested with Liberase (Roche) and type I DNase in serum-free RPMI media at 37°C for 45 min. Immune cells were isolated after gradient centrifugation from a 37:70% Percoll interface and washed twice with staining buffer. Immune cells were stained with directly conjugated antibodies specific to CD3, CD8, CD4, CD95, CD127, KLRG1, CD44, and CD262 (all reagents from eBioscience); and CD120a and CD120b (from BioLegend). WNV-specific $CD8^+$ T cells were identified using a tetramer derived from an NS4b peptide restricted to the MHC class I D^b allele (produced at the immune monitoring core facility at the Fred Hutchinson Cancer Research Center, Seattle) directly conjugated to either phycoerythrin (PE) or allophycocyanin (APC). Annexin V^+ staining was performed according to the manufacturer's instructions (BD Biosciences). Pacific Blue-conjugated Annexin V^+ (BioLegend) or fluorescein isothiocyanite (FITC)-conjugated Annexin V^+ (BD Biosciences) was used for staining. Intracellular FoxP3 staining to identify regulatory T cells was performed as previously described (Lund et al., 2008; Suthar et al., 2010). Intracellular IFN-γ and TNF-α staining was performed on splenocytes as previous described (Suthar et al., 2010). In brief, lymphocytes were stimulated with 1 μg/ml of the WNV NS4b peptide (SSVWNATTAI) or LCMV-GP33 ($GP_{33–41}$) for 4 hr at 37°C. Cells were washed and stained for cell surface markers followed by permeabilization-fixation using the Cytofix-Cytoperm Kit (BD Pharmingen) and stained with a Pacific Blue-conjugated IFN-γ and a FITC-conjugated TNF-α antibody (eBioscience) at 4°C for 30 min, washed, and analyzed by flow cytometry. Caspase activity was measured using the Vybrant FAM Caspase-3 and -7 or Caspase-8 Assay Kit (Invitrogen), according to the manufacturer's instructions. For detection of intracellular Bcl-2, cells were fixed and treated with the FoxP3 intracellular staining kit (eBioscience) followed by staining with an APC-conjugated Bcl-2 antibody (BioLegend). For detection of Bim and Bcl-xL, cells were fixed for 10 min with 4% paraformaldehyde at room temperature, permeabilized with 0.1% saponin for 30 min on ice, and stained with Bim (Cell Signaling), Bcl-xL (Clone 54H6; Cell Signaling), and isotype control (Rabbit IgG mAb clone DA1E) antibody for 30 min on ice. Alexa Fluor 488-conjugated (Cell Signaling) secondary antibody was used at a dilution of 1:1,000, and cells were analyzed by flow cytometry. For measurement of $CD8^+$ T cell proliferation in vivo, mice were injected with 1 mg of BrdU for 6 hr via the intraperitoneal route, and splenocytes were stained with CD8, PE-conjugated NS4b tetramer, and APC-conjugated BrdU, according to the manufacturer's instructions. Flow cytometry was performed on a BD LSRII machine using BD FACSDiva software. Cell analysis was performed on FlowJo (v8.7.2) software.

Analysis of TNF-α-, TRAIL-, and CD95L-Mediated Cell Death

For TNF-α and TRAIL treatments, splenocytes from recipient *Rag1*$^{-/-}$ infected mice were resuspended in cRPMI and cultured at 37°C for 6 hr with either 2 ng/ml TNF-α or 20 ng/ml Super*Killer*TRAIL (Enzo Life Sciences). For CD95L treatment, splenocytes were cultured at 37°C for 3 hr with 250 ng/ml FLAG-tagged recombinant CD95L (Alexis Biochemicals) crosslinked by 4 μg/ml M2 monoclonal anti-FLAG antibody (Sigma-Aldrich). Cells were stained and analyzed for cell death (Annexin V^+) by flow cytometry.

Ex Vivo TCR Stimulation

$CD8^+$ T cells were isolated directly from WT and *Dhx58*$^{-/-}$ splenocytes using the negative selection $CD8^+$ T Cell Isolation Kit (Miltenyi Biotec) according to the manufacturer's instructions. For ex vivo TCR stimulation, 96-well plates were precoated overnight with 1 μg/ml anti-CD3 (BioLegend) and 5 μg/ml anti-CD28 (BioLegend). Isolated $CD8^+$ T cells were plated (6×10^5 cells per well) in 200 μl cRPMI media supplemented with 500 IU/ml of murine IL-2.

Statistical Analysis

For in vitro studies and immune cell analysis, an unpaired Student's t test was used to determine statistical differences. For in vivo viral-burden analysis, Mann-Whitney analysis was used to determine statistical differences. Kaplan-Meier survival curves were analyzed by the log-rank test. A p value $\leq$ 0.05 was considered statistically significant. All data were analyzed using Prism software (GraphPad Prism5).

SUPPLEMENTAL INFORMATION

Supplemental Information includes four figures and one table and can be found with this article online at http://dx.doi.org/10.1016/j.immuni.2012.07.004.

ACKNOWLEDGMENTS

We thank S. Thomas and M. Kaja for helpful discussion. We thank B. Doehle and S. Horner for comments and manuscript revisions. Work was supported by National Institutes of Health grants 1F32AI081490, R01AI074973, U19AI083019, and U54AI081680.

Received: November 18, 2011
Revised: April 13, 2012
Accepted: April 27, 2012
Published online: July 26, 2012

REFERENCES

Aggarwal, B.B. (2003). Signalling pathways of the TNF superfamily: a double-edged sword. Nat. Rev. Immunol. *3*, 745–756.

Brien, J.D., Uhrlaub, J.L., and Nikolich-Zugich, J. (2007). Protective capacity and epitope specificity of CD8(+) T cells responding to lethal West Nile virus infection. Eur. J. Immunol. *37*, 1855–1863.

Brien, J.D., Uhrlaub, J.L., and Nikolich-Zugich, J. (2008). West Nile virus-specific CD4 T cells exhibit direct antiviral cytokine secretion and cytotoxicity and are sufficient for antiviral protection. J. Immunol. *181*, 8568–8575.

Brien, J.D., Daffis, S., Lazear, H.M., Cho, H., Suthar, M.S., Gale, M., Jr., and Diamond, M.S. (2011). Interferon regulatory factor-1 (IRF-1) shapes both innate and CD8(+) T cell immune responses against West Nile virus infection. PLoS Pathog. *7*, e1002230.

Centers for Disease Control and Prevention (CDC). (2008). West Nile virus activity–United States, 2007. MMWR. Morb. Mortal. Wkly. Rep. *57*, 720–723.

Daffis, S., Samuel, M.A., Suthar, M.S., Keller, B.C., Gale, M., Jr., and Diamond, M.S. (2008). Interferon regulatory factor IRF-7 induces the antiviral alpha interferon response and protects against lethal West Nile virus infection. J. Virol. *82*, 8465–8475.

Diamond, M.S., Shrestha, B., Marri, A., Mahan, D., and Engle, M. (2003a). B cells and antibody play critical roles in the immediate defense of disseminated infection by West Nile encephalitis virus. J. Virol. *77*, 2578–2586.

Diamond, M.S., Sitati, E.M., Friend, L.D., Higgs, S., Shrestha, B., and Engle, M. (2003b). A critical role for induced IgM in the protection against West Nile virus infection. J. Exp. Med. *198*, 1853–1862.

Fredericksen, B.L., Keller, B.C., Fornek, J., Katze, M.G., and Gale, M., Jr. (2008). Establishment and maintenance of the innate antiviral response to

West Nile Virus involves both RIG-I and MDA5 signaling through IPS-1. J. Virol. *82*, 609–616.

Gelman, A.E., Zhang, J., Choi, Y., and Turka, L.A. (2004). Toll-like receptor ligands directly promote activated CD4+ T cell survival. J. Immunol. *172*, 6065–6073.

Grandvaux, N., Servant, M.J., tenOever, B., Sen, G.C., Balachandran, S., Barber, G.N., Lin, R., and Hiscott, J. (2002). Transcriptional profiling of interferon regulatory factor 3 target genes: direct involvement in the regulation of interferon-stimulated genes. J. Virol. *76*, 5532–5539.

Grayson, J.M., Zajac, A.J., Altman, J.D., and Ahmed, R. (2000). Cutting edge: increased expression of Bcl-2 in antigen-specific memory CD8+ T cells. J. Immunol. *164*, 3950–3954.

Havenar-Daughton, C., Kolumam, G.A., and Murali-Krishna, K. (2006). Cutting Edge: The direct action of type I IFN on CD4 T cells is critical for sustaining clonal expansion in response to a viral but not a bacterial infection. J. Immunol. *176*, 3315–3319.

Janssen, E.M., Droin, N.M., Lemmens, E.E., Pinkoski, M.J., Bensinger, S.J., Ehst, B.D., Griffith, T.S., Green, D.R., and Schoenberger, S.P. (2005). CD4+ T-cell help controls CD8+ T-cell memory via TRAIL-mediated activation-induced cell death. Nature *434*, 88–93.

Joshi, N.S., Cui, W., Chandele, A., Lee, H.K., Urso, D.R., Hagman, J., Gapin, L., and Kaech, S.M. (2007). Inflammation directs memory precursor and short-lived effector CD8(+) T cell fates via the graded expression of T-bet transcription factor. Immunity *27*, 281–295.

Kato, H., Takeuchi, O., Sato, S., Yoneyama, M., Yamamoto, M., Matsui, K., Uematsu, S., Jung, A., Kawai, T., Ishii, K.J., et al. (2006). Differential roles of MDA5 and RIG-I helicases in the recognition of RNA viruses. Nature *441*, 101–105.

Keller, B.C., Fredericksen, B.L., Samuel, M.A., Mock, R.E., Mason, P.W., Diamond, M.S., and Gale, M., Jr. (2006). Resistance to alpha/beta interferon is a determinant of West Nile virus replication fitness and virulence. J. Virol. *80*, 9424–9434.

Kolumam, G.A., Thomas, S., Thompson, L.J., Sprent, J., and Murali-Krishna, K. (2005). Type I interferons act directly on CD8 T cells to allow clonal expansion and memory formation in response to viral infection. J. Exp. Med. *202*, 637–650.

Komuro, A., and Horvath, C.M. (2006). RNA and Virus-Independent Inhibition of Antiviral Signaling by RNA Helicase LGP2. J.Virol. *80*, 12332–12342.

Li, S., Wang, L., Berman, M., Kong, Y.Y., and Dorf, M.E. (2011). Mapping a dynamic innate immunity protein interaction network regulating type I interferon production. Immunity *35*, 426–440.

Loo, Y.M., Fornek, J., Crochet, N., Bajwa, G., Perwitasari, O., Martinez-Sobrido, L., Akira, S., Gill, M.A., García-Sastre, A., Katze, M.G., and Gale, M., Jr. (2008). Distinct RIG-I and MDA5 signaling by RNA viruses in innate immunity. J. Virol. *82*, 335–345.

Lund, J.M., Hsing, L., Pham, T.T., and Rudensky, A.Y. (2008). Coordination of early protective immunity to viral infection by regulatory T cells. Science *320*, 1220–1224.

Michalek, R.D., and Rathmell, J.C. (2010). The metabolic life and times of a T-cell. Immunol. Rev. *236*, 190–202.

Pulendran, B., and Ahmed, R. (2011). Immunological mechanisms of vaccination. Nat. Immunol. *12*, 509–517.

Purtha, W.E., Myers, N., Mitaksov, V., Sitati, E., Connolly, J., Fremont, D.H., Hansen, T.H., and Diamond, M.S. (2007). Antigen-specific cytotoxic T lymphocytes protect against lethal West Nile virus encephalitis. Eur. J. Immunol. *37*, 1845–1854.

Quigley, M., Martinez, J., Huang, X., and Yang, Y. (2009). A critical role for direct TLR2-MyD88 signaling in CD8 T-cell clonal expansion and memory formation following vaccinia viral infection. Blood *113*, 2256–2264.

Rahman, A.H., Cui, W., Larosa, D.F., Taylor, D.K., Zhang, J., Goldstein, D.R., Wherry, E.J., Kaech, S.M., and Turka, L.A. (2008). MyD88 plays a critical T cell-intrinsic role in supporting CD8 T cell expansion during acute lymphocytic choriomeningitis virus infection. J. Immunol. *181*, 3804–3810.

Rothenfusser, S., Goutagny, N., DiPerna, G., Gong, M., Monks, B.G., Schoenemeyer, A., Yamamoto, M., Akira, S., and Fitzgerald, K.A. (2005). The RNA helicase Lgp2 inhibits TLR-independent sensing of viral replication by retinoic acid-inducible gene-I. J. Immunol. *175*, 5260–5268.

Saito, T., Hirai, R., Loo, Y.M., Owen, D., Johnson, C.L., Sinha, S.C., Akira, S., Fujita, T., and Gale, M., Jr. (2007). Regulation of innate antiviral defenses through a shared repressor domain in RIG-I and LGP2. Proc. Natl. Acad. Sci. USA *104*, 582–587.

Samuel, M.A., and Diamond, M.S. (2006). Pathogenesis of West Nile Virus infection: a balance between virulence, innate and adaptive immunity, and viral evasion. J. Virol. *80*, 9349–9360.

Samuel, M.A., Whitby, K., Keller, B.C., Marri, A., Barchet, W., Williams, B.R., Silverman, R.H., Gale, M., Jr., and Diamond, M.S. (2006). PKR and RNase L contribute to protection against lethal West Nile Virus infection by controlling early viral spread in the periphery and replication in neurons. J. Virol. *80*, 7009–7019.

Sarkar, D., Desalle, R., and Fisher, P.B. (2008). Evolution of MDA-5/RIG-I-dependent innate immunity: independent evolution by domain grafting. Proc. Natl. Acad. Sci. USA *105*, 17040–17045.

Satoh, T., Kato, H., Kumagai, Y., Yoneyama, M., Sato, S., Matsushita, K., Tsujimura, T., Fujita, T., Akira, S., and Takeuchi, O. (2010). LGP2 is a positive regulator of RIG-I- and MDA5-mediated antiviral responses. Proc. Natl. Acad. Sci. USA *107*, 1512–1517.

Shrestha, B., and Diamond, M.S. (2004). Role of CD8+ T cells in control of West Nile virus infection. J. Virol. *78*, 8312–8321.

Shrestha, B., Samuel, M.A., and Diamond, M.S. (2006). CD8+ T cells require perforin to clear West Nile virus from infected neurons. J. Virol. *80*, 119–129.

Sitati, E.M., and Diamond, M.S. (2006). CD4+ T-cell responses are required for clearance of West Nile virus from the central nervous system. J. Virol. *80*, 12060–12069.

Suthar, M.S., Ma, D.Y., Thomas, S., Lund, J.M., Zhang, N., Daffis, S., Rudensky, A.Y., Bevan, M.J., Clark, E.A., Kaja, M.K., et al. (2010). IPS-1 is essential for the control of West Nile virus infection and immunity. PLoS Pathog. *6*, e1000757.

Szretter, K.J., Daffis, S., Patel, J., Suthar, M.S., Klein, R.S., Gale, M., Jr., and Diamond, M.S. (2010). The innate immune adaptor molecule MyD88 restricts West Nile virus replication and spread in neurons of the central nervous system. J. Virol. *84*, 12125–12138.

Thompson, L.J., Kolumam, G.A., Thomas, S., and Murali-Krishna, K. (2006). Innate inflammatory signals induced by various pathogens differentially dictate the IFN-I dependence of CD8 T cells for clonal expansion and memory formation. J. Immunol. *177*, 1746–1754.

Tourneur, L., and Chiocchia, G. (2010). FADD: a regulator of life and death. Trends Immunol. *31*, 260–269.

Venkataraman, T., Valdes, M., Elsby, R., Kakuta, S., Caceres, G., Saijo, S., Iwakura, Y., and Barber, G.N. (2007). Loss of DExD/H box RNA helicase LGP2 manifests disparate antiviral responses. J. Immunol. *178*, 6444–6455.

Wilkins, C., and Gale, M., Jr. (2010). Recognition of viruses by cytoplasmic sensors. Curr. Opin. Immunol. *22*, 41–47.

Yoneyama, M., Kikuchi, M., Matsumoto, K., Imaizumi, T., Miyagishi, M., Taira, K., Foy, E., Loo, Y.M., Gale, M., Jr., Akira, S., et al. (2005). Shared and unique functions of the DExD/H-box helicases RIG-I, MDA5, and LGP2 in antiviral innate immunity. J. Immunol. *175*, 2851–2858.

Zhang, N., and Bevan, M.J. (2010). Dicer controls CD8+ T-cell activation, migration, and survival. Proc. Natl. Acad. Sci. USA *107*, 21629–21634.

Zhang, N., Hartig, H., Dzhagalov, I., Draper, D., and He, Y.W. (2005). The role of apoptosis in the development and function of T lymphocytes. Cell Res. *15*, 749–769.

Zhao, Y., De Trez, C., Flynn, R., Ware, C.F., Croft, M., and Salek-Ardakani, S. (2009). The adaptor molecule MyD88 directly promotes CD8 T cell responses to vaccinia virus. J. Immunol. *182*, 6278–6286.

Zou, J., Chang, M., Nie, P., and Secombes, C.J. (2009). Origin and evolution of the RIG-I like RNA helicase gene family. BMC Evol. Biol. *9*, 85.